Deuterium Solvent Isotope Effect and Proton-Inventory Studies of Factor Xa-Catalyzed Reactions†

Daoning Zhang§ and Ildiko M. Kovach*

Department of Chemistry, The Catholic University of America, 620 Michigan Avenue, Washington, D.C. 20064

Received June 19, 2006; Revised Manuscript Received September 20, 2006

ABSTRACT: Kinetic solvent isotope effects (KSIEs) for the factor Xa (FXa)-catalyzed activation of prothrombin in the presence and absence of factor Va (FVa) and 5.0×10^{-5} M phospholipid vesicles are slightly inverse, 0.82−0.93, when substrate concentrations are at 0.2 K_m. This is consistent with the rate-determining association of the enzyme−prothrombin assembly, rather than the rate-limiting chemical transformation. FVa is known to effect a major conformational change to expose the first scissile bond in prothrombin, which is the likely event triggering a major solvent rearrangement. At prothrombin concentrations > 5 K_m, the KSIE is 1.6 ± 0.3, when FXa is in a 1:1 ratio with FVa but becomes increasingly inverse, 0.30 ± 0.05 and 0.19 ± 0.04, when FXa/FVa is 1:4, with an increasing FXa and substrate concentration. The rate-determining step changes with the conditions, but the chemical step is not limiting under any circumstance. This corroborates the proposed predominance of the meizothrombin pathway when FXa is well-saturated with the prothrombin complex. In contrast, the FXa-catalyzed hydrolysis of N-α-*Z*-D-Arg-Gly-Arg-pNA·2HCl (S-2765) and H-D-Ile-L-Pro-L-Arg-pNA·HCl (S-2288) is most consistent with two-proton bridges forming at the transition state between Ser^{195} OγH and His^{57} Nϵ2 and His^{57} Nδ1 and Asp^{102} COOβ^- at the active site, with transition-state fractionation factors of $\phi_1 = \phi_2 = 0.57 \pm 0.07$ and $\phi_S = 0.78 \pm 0.16$ for solvent rearrangement for S-2765 and $\phi_1 = \phi_2 = 0.674 \pm 0.001$ for S-2288 under enzyme saturation with the substrate at pH 8.40 and 25.0 ± 0.1 °C. The rate-determining step(s) in these reactions is most likely the cleavage of the C−N bond and departure of the leaving group.

Factor Xa (FXa)[1] is one of the best characterized of the serine proteases in the cardiovascular system (*1*−*6*). It catalyzes the efficient activation of a large precursor protein, prothrombin, to form α-thrombin (*1*, *7*, *8*). Although several proteolytic enzymes can bring about this reaction, it is FXa that performs this key function under physiological conditions. On the basis of extensive investigations, the prothrombin complex is known to consist of phospholipid surface, prothrombin, Ca^{2+}, and factor Va (FVa) (*8*−*12*). This construct facilitates the activation of prothrombin by ~3×10^5-fold over catalysis by FXa alone (*13*, *14*). The activation of human prothrombin involves the hydrolysis of two peptide bonds, Arg^{322}−Ile^{323} followed by Arg^{273}−Thr^{274}. In contrast, when FXa acts alone, bond cleavage occurs in the opposite order. Different intermediates are formed in the two pathways that have also been studied independently (*9*, *14*). More in-depth kinetic studies lately revealed that an appreciable fraction of prothrombin is channeled directly to the thrombin product without releasing intermediate products (*14*).

FXa activation of prothrombin without FVa is inadequate for survival. FVa itself is processed from FV by cleavage, catalyzed by (human) thrombin at Arg^{709} into a heavy and light chain (*10*). Both chains are required for the interaction with FXa, but only the heavy chain binds prothrombin without Ca^{2+} (*11*). The binding sites for FXa and prothrombin have been located in the middle section (*11*) and the COOH terminus (*12*) of the heavy chain of FVa, respectively (*15*). In fact, an exosite of FXa, which is exposed upon the interaction with FVa for prothrombin tethering, seems to contain amino acids near the active site of the enzyme. This can serve to provide optimal docking of the scissile bonds of prothrombin. The crystal structures of meizothrombin desF1 and prothrombin-2 show the two prothrombin cleavage sites at 36 Å apart (*16*). For prothrombin to be cleaved at Arg^{322}, a rotation around the Gly^{319} and Gly^{324} hinge points has to occur. The rate of cleavage at the second site is not affected much by the presence of FVa (*11*).

Similar to other proteases (*17*), FXa uses a general-base catalytic apparatus (the catalytic triad), in addition to an oxyanion hole and an elaborate binding site for prothrombin. Deuterium kinetic solvent isotope effects (KSIEs) (*18*−*22*) have been used to establish the occurrence of proton bridges at the rate-determining transitions state(s) (TSs) in biological general-acid−base-catalyzed reactions (*23*). An extension of the KSIE studies to partial solvent isotope effects or proton inventories has provided additional information on the

† This work was supported in part by the U.S. National Institutes of Health, Grant number 1 R15 HL067754-01.

* To whom correspondence should be addressed. Telephone: (202) 319-6550. Fax: (202) 319-5381. E-mail: kovach@cua.edu.

§ Current address: Center for Biomolecular Structure and Organization, Department of Chemistry and Biochemistry, University of Maryland, College Park, MD 20742-3360.

[1] Abbreviations: APC, activated protein C; FXa, factor Xa; FVa, factor Va; KSIE, kinetic solvent isotope effect; LUV, large unilammellar vesicle; OD, optical density; PC, protein C; pNA, *para*-nitroaniline; PCh, phosphatidylcholine; PS, phosphatidylserine; RS, reactant state; S-2765, N-α-*Z*-D-Arg-Gly-Arg-pNA·2HCl; S-2288, H-D-Ile-L-Pro-L-Arg-pNA·HCl; S-2238, H-D-Phe-Pip-Arg-pNA; SSHB, short strong hydrogen bond; TLC, thin-layer chromatography; TS, transition state.

10.1021/bi061218m CCC: $33.50
Published on Web 11/07/2006

number and nature of proton bridges at the rate-determining TSs. Proton inventories are measured in mixtures of buffered light and heavy water (*18*−*22*, *24*−*29*).

A close relative of FXa is α-thrombin, the product of FXa catalysis and the central enzyme in the blood cascade. We have in the recent past presented conclusions from the analysis of proton-inventory data obtained on the human α-thrombin-catalyzed hydrolysis of natural substrates and oligopeptide mimics of them (*30*, *31*). In thrombin-catalyzed reactions, as in the pancreatic proteases, multiproton catalysis pertains to proton bridges between Nϵ2 of His^{57} and the OγH of Ser^{195} and Nδ1 of His^{57} and COOβ^- of Asp^{102} at the active site (*23*, *31*). We carried out proton-inventory experiments for the human α-thrombin-catalyzed activation of fibrinogen into fibrinopeptide A, the formation of fibrin colloid, and the human α-thrombin-catalyzed activation of protein C (PC) to activated protein C (APC) (*30*). The proton inventories for fibrinogen activation are bowl-shaped and are most consistent with two proton bridges forming at the TS of the chemical process at all substrate concentrations. In contrast, the activation of PC gives KSIEs slightly inverse at substrate concentrations below K_m, indicating the dominance of physical rather than chemical steps limiting the rate under these conditions.

The effect of P-site interactions with S-binding sites on protease enzymes has been established by a variety of studies, including proton inventories. The last of these was our study of thrombin-catalyzed reactions of oligopeptide substrates (*31*). When the requisite number and kind of P−S site interactions are present, the hydrogen-bonding distance between proton acceptors and donors of the catalytic triad contracts at the rate-determining TS. We have also shown that the hallmark of the effect of P′ residues in leaving-group departure is a conformational change associated with a major rearrangement of solvating water. In thrombin-catalyzed reactions, a net increase occurs in the isotopic fractionation factors for hydrogen bonds at solvation sites in the rate-determining step. This effect is elicited by interactions at the binding site of the leaving group or substrate specificity site. This observation is well supported by other studies of P′-site interactions in catalysis by (*32*−*34*) and inhibition of (*35*) proteases. The proton-inventory technique has been particularly revealing about the importance of solvent reorganization in substrate binding and leaving-group release in thrombin-catalyzed reactions.

The premise of this endeavor has been that association and rearrangement of the FXa−prothrombin assembly are likely to limit the rate at the aqueous−lipid interface, because the very role of activation on heterogeneous surfaces is the facilitation of chemical transformation by juxtaposing and binding reactant partners. The process is associated with solvent restructuring, and thus, the physiological reaction catalyzed by FXa is likely to show a strong contribution from solvent rearrangement. Indeed, the activation of prothrombin by FXa gave inverse KSIEs that approached 0.2−0.3 in the presence of FXa/FVa in a 1:4 ratio and 50 μM phospholipid vesicles (LUV), as the substrate concentrations were raised above K_m, indicating the dominance of physical rather than chemical steps limiting the rate at the aqueous−lipid interface. In the presence of FXa/FVa = 1:1 and at enzyme saturation with the substrate, however, the KSIEs became small normal, i.e., greater than 1.0. To obtain an unmasked picture of the rate-determining events in peptide-bond hydrolysis catalyzed by FXa, we also studied proven mimics of the natural substrates with the proton-inventory technique. FXa-catalyzed reactions of chromogenic substrates behaved similarly to the thrombin-catalyzed reactions of oligopeptide *p*-nitroanilides or 4-methyl umbelliferones, i.e., showed two-proton bridges at the rate-determining TS. However, N-α-*Z*-D-Arg-Gly-Arg-pNA·2HCl, a very efficient substrate of FXa, hydrolyzed with a contribution from solvent rearrangement at the rate-determining TS while saturating the enzyme. Solvent restructuring is likely to accompany leaving-group departure, which then is part of the rate-determining process.

Once more, the results of KSIE and proton-inventory studies bring to light the critical importance of the participation of proton bridges and water structure in catalysis of another key serine protease, FXa.

EXPERIMENTAL PROCEDURES

Materials. Anhydrous dimethyl sulfoxide (DMSO), heavy water with 99.9% deuterium content, and anhydrous methanol were purchased from Aldrich Chemical Co. All buffer salts were reagent-grade and were purchased from Aldrich, Fisher, or Sigma Chemical Co. Solid bovine FXa, molecular mass of 45 300 Da, 0.8 unit/mg in powder and Soybean Trypsin inhibitor (STI), 20 μg/mL, were purchased from Sigma Chemical Co. N-α-*Z*-D-Arg-Gly-Arg-4-*para*-nitroaniline (pNA)·2HCl (S-2765), 99% thin-layer chromatography (TLC), H-D-Ile-L-Pro-L-Arg-pNA·HCl (S-2288), 99% (TLC), and H-D-Phe-Pip-Arg-pNA (S-2238), 99% (TLC), were purchased from Diapharma Group, Inc. Human FXa, molecular mass of 46 000 Da, 7.7 mg/mL in 50% glycerol/H_2O, FVa, molecular mass of 168 000 Da, 2190 units/mg in 50% glycerol/H_2O and 2 mM $CaCl_2$, and prothrombin were purchased from Haematologic Technologies, Inc. Human α-thrombin, molecular mass of 36 500 Da, 3010 NIH units/mg in pH 6.5, 0.05 M sodium citrate buffer, 0.2 M NaCl, and 0.1% poly(ethylene glycol) (PEG)-8000 was purchased from Enzyme Research Laboratories. The Na^+ salt of L-phosphatidylserine (PS) from brain and a chloroform solution of L-phosphatidylcholine (PCh) from eggs were purchased from Avanti Polar Lipids, Inc.

Instruments and Solutions. Spectroscopic measurements and the preparation of solutions were as described earlier (*31*). Buffers were prepared by weight from Tris-base and Tris-HCl in the pH range of 7.1−9.1 in freshly distilled deionized or heavy water to contain 0.020 M Tris, 0.15−0.30 M NaCl, 0.1% PEG-4000, and 5×10^{-3} M $CaCl_2$.

Active-Site Concentrations. The same stock solution was used for all experiments on the same day with intermittent checking of activity with S-2765. FXa concentrations were calculated from similar determinations using S-2765 as the substrate and $k_{cat} = 240$ s^{-1} at 25 °C (Diapharma catalog). There was no background hydrolysis of the substrates in the absence of the enzyme, and the slopes were proportional to the FXa concentration within 90% of the values calculated from weights, as indicated by the provider.

Prothrombin Activation Catalyzed by Human FXa. Phospholipid vesicles (LUV) were prepared according to well-tested methods (*36*, *37*) from 50 μL of 25 mg/mL PCh and 50 μL of 10 mg/mL PS, mixed, and dried under He gas. The dried lipids, 1.75 mg, were then dissolved in 4 mL of

pH 7.50 buffer and 0.15 M NaCl (Ca^{2+} free) to reach a final concentration of 560 μM. This stock solution was stored frozen and diluted to 56 μM LUV, followed by extrusion before use.

For pseudo-first-order kinetic studies, a 5.0 μM prothrombin solution was prepared from a stock solution (25 μM) by dilution using pH 7.50 buffer containing 5×10^{-3} M $CaCl_2$. For prothrombin activation in the presence of LUV, 355 μL of 56 μM LUV was added to a 5 μL solution of 25 nM FXa and 100 nM FVa to attain a final concentration of 0.33 nM FXa. The mixture was incubated at 25.0 ± 0.1 °C for 15 min and 15 μL of 5.0 μM prothrombin, to reach 0.20 μM in the prothrombin complex (360 μL), initiated the reaction. Reactions were also carried out with higher FXa concentrations and at different prothrombin concentrations but in the absence of FVa and LUV.

For initial rate measurements, 41.7 nM FXa (FXa/FVa = 1:4) in pH 7.50 buffer, 0.15 M NaCl, and 5×10^{-3} M $CaCl_2$ was prepared with 56 μM LUV, aliquoted at 10 μL volume, and kept at −20 °C. Prior to the reaction, 10 μL of FXa solution was mixed with 110 μL of 56 μM LUV and incubated at 25.0 ± 0.1 °C for 15 min. The reaction was initiated by adding 5 μL of 100 μM prothrombin solution to obtain 4.0 μM prothrombin and 3.3 nM FXa in the prothrombinase complex solution. Reactions were also carried out at different FVa concentrations and different prothrombin concentrations at 50 μM LUV. In all cases, an aliquot of 20 μL was drawn at different time intervals to test the amidolytic activity of thrombin produced. The sample was added to 715 μL of pH 7.50 buffer and 0.15 M NaCl and preincubated in a cell at 25.0 ± 0.1 °C for 10 min. A total of 15 μL of 3.2×10^{-3} M S-2238 in pH 7.5 buffer containing 900 nM Soybean trypsin inhibitor and 0.15 M NaCl was added to the solution to start the hydrolysis, and pNA release was monitored for 1 min at 405 nm. The thrombin concentration was calculated from the average of slopes of three to five parallel runs and the k_{cat} value for S-2238 (*31*). Repeats from several fresh LUV preparations gave values within 10% error. Prothrombin conversion to thrombin occurred near 90%.

FXa-Catalyzed Hydrolysis of Chromogenic Substrates. The FXa-catalyzed hydrolysis at the pH plateau, in buffers at pH 8.40 and equivalent pL (L = H or D), 0.30 M NaCl, 5×10^{-3} M $CaCl_2$, and 0.1% PEG-4000 at 25.0 ± 0.1 °C, of S-2288 and S-2765, were monitored at 405 nm, $\epsilon = 9420 \pm 101$ optical density (OD) M^{-1}, or 445 nm, $\epsilon = 1245 \pm 16$ OD M^{-1}, for the release of p-NA. In all measurements, the enzyme solution was added from the same aqueous stock solution in 0.5−2% of the total volume of 1.0 mL to the isotopic buffer in a cuvette. The mixture was prethermostated for 10−15 min at the working temperature, and the reaction was initiated by the injection of 20 μL of substrate solution in DMSO. Initial rates of substrate hydrolysis were calculated from 100 to 1000 absorbance readings at 405 nm in 1 min, and first-order or full-progress curves contained 1000 points. Good pseudo-first-order behavior was observed at >95% completion of the reaction (k_{cat}/K_m).

The reactions were carried out in 0.5 or 1.0 mL volumes containing 1.9×10^{-9} M bovine FXa, S-2288 concentrations between 1.30×10^{-4} and 3.46×10^{-3} M ($K_m = 1.7 \times 10^{-3}$ M) for determining Michaelis−Menten parameters and at 2.88×10^{-3} M for proton-inventory studies using initial velocity measurements. The human FXa-catalyzed hydrolysis of S-2765 was studied at 14.5×10^{-9} M FXa and 1.0×10^{-3} M substrate ($K_m = 2.6 \times 10^{-4}$ M) in full-progress curves and at 7.3×10^{-9} M FXa and 2.0×10^{-5} M substrate for pseudo-first-order kinetics.

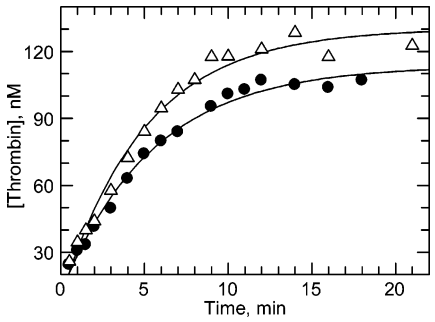

FIGURE 1: Time dependence of human FXa-catalyzed human prothrombin activation in the presence of 4-fold excess of FVa, at pH 7.50, 0.020 M Tris buffer, 5.0×10^{-5} M LUV, 5×10^{-3} M $CaCl_2$, and 25.0 ± 0.1 °C. (●) H_2O buffer, and (△) D_2O buffer.

Analysis of Kinetic and Proton-Inventory Data. The integrated Michaelis−Menten equation (*38*)

$$((A - A_o)/\epsilon k_{cat}[E]) + K_m/k_{cat}(\ln(A_{inf} - A_o)/(A_{inf} - A)) = t$$

where A, A_o, and A_{inf} are the absorbance values at time t, 0, and infinity, respectively, ϵ is the molar absorbtivity, [E] is the enzyme concentration, and k_{cat} and K_m are the Michaelis−Menten parameters, was fitted to two sets of 1000 data points from full-progress curves for the FXa-catalyzed hydrolysis of S-2765. The calculated k_{cat} values for the reaction in each of the nine isotopic buffers were used for constructing the proton-inventory curve. The Michaelis−Menten parameters calculated were in good agreement with initial estimates from the first 10−50 data points and with published values under similar conditions. All data reductions using predefined and custom-defined equations were performed using the GraFit 3.0 and 5.0 software (*39*).

RESULTS

Activation of Prothrombin. FXa-catalyzed prothrombin activation occurs on membrane surfaces *in vivo*. The success of the reaction and the extent of prothrombin conversion to thrombin or meizothrombin *in vitro* greatly depend upon the nature and concentrations of LUV and the auxiliary protein, FVa (*7*, *36*, *37*, *40*). Whereas the yield of prothrombin conversion to thrombin appears to increase with the concentration of LUV (composed of PS and PCh as described in the Experimental Procedures), at least up to 2×10^{-3} M PS/PC, the rate of the reaction is maximal around 5×10^{-5} M (*36*, *37*). We measured KSIEs predominantly under these conditions and at FXa/FVa = 1:4. This FXa/FVa ratio was reported to be optimal, and the K_m value under these conditions is $\sim 10^{-6}$ M (*37*, *40*). A total of 40−60% of prothrombin has been shown to convert to thrombin via meizothrombin under these conditions (*36*, *37*). The time-dependent production of thrombin was monitored by the amidolytic assay.

Pseudo-first-order kinetics were observed at prothrombin concentrations $< 2 \times 10^{-7}$ M [~ 0.2 K_m (*37*, *40*)] at FXa/FVa = 1:4, shown in Figure 1. The conditions and the k_{cat}/K_m value are in the first column in Table 1A. Similarly, pseudo-first-order rate constants were measured in the

Table 1: Solvent Isotope Effects for Human FXa-Catalyzed Human Prothrombin Activation at pH 7.50 in 0.020 M Tris Buffer and 25.0 ± 0.1 °C

		A. Pseudo-first-Order Kinetics		
10^6 [LUV] (M)	50	50		
10^9 [FXa] (M)	0.33	10	93	493
10^9 [FVa] (M)	1.3			
10^6 [prothrombin] (M)	0.20	0.30	4.1	25
k_{cat}/K_m (H) (M^{-1} s^{-1})	$(7.6 \pm 1.2) \times 10^6$	$(3.9 \pm 0.2) \times 10^4$	164 ± 9	62 ± 2
k_{cat}/K_m (D) (M^{-1} s^{-1})	$(9.0 \pm 1.7) \times 10^6$	$(4.8 \pm 0.3) \times 10^4$	188 ± 9	66 ± 1
KSIE	0.84 ± 0.22	0.82 ± 0.07	0.87 ± 0.06	0.93 ± 0.04
		B. Initial Rate Method		
10^6 [LUV] (M)	50	50	50	50
10^9 [FXa] (M)	0.33	0.33	1.0	15
10^9 [FVa] (M)	1.3	1.3	1.0	
10^6 [prothrombin] (M)	6.8	4.0	4.0	9.9
k_{cat} (H) (s^{-1})	0.31 ± 0.05	0.67 ± 0.01	0.28 ± 0.05	$(1.74 \pm 0.20) \times 10^{-3}$
k_{cat} (D) (s^{-1})	1.6 ± 0.2	2.2 ± 0.2	0.18 ± 0.01	$(2.53 \pm 0.14) \times 10^{-3}$
KSIE	0.19 ± 0.04	0.30 ± 0.05	1.56 ± 0.31	0.69 ± 0.09

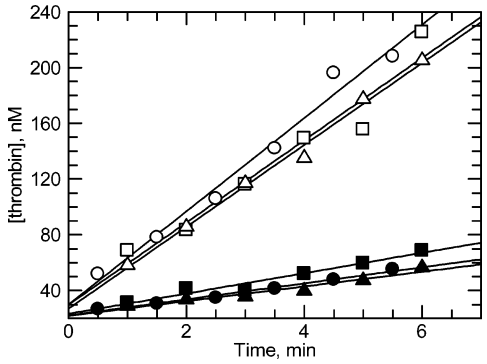

FIGURE 2: Initial rates of human FXa-catalyzed human prothrombin activation in the presence of 4-fold excess of FVa, at pH 7.50, 0.020 M Tris buffer, 5.0×10^{-5} M LUV, 5×10^{-3} M $CaCl_2$, and 25.0 ± 0.1 °C. (●, ■, and ▲) H_2O, and (○, □, and △) D_2O.

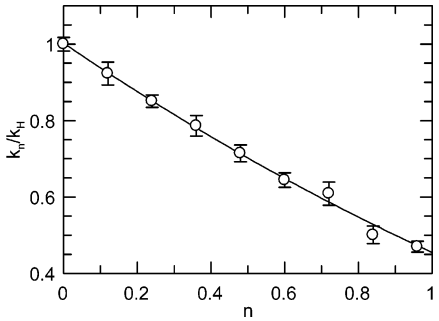

FIGURE 3: Ratios of initial rates measured in mixed isotopic solvents over the initial rates measured in water plotted against the atom fraction of deuterium, *n*, for bovine FXa-catalyzed S-2288 (at >2 K_m) hydrolysis at pH 8.40 and equivalent pL, 0.020 M Tris buffer, 0.30 M NaCl, 5×10^{-3} M $CaCl_2$, 0.1% PEG-4000, and 2% DMSO at 25.0 ± 0.1 °C. The equation of the line is $k_n/k_H = 1.0(1 - n + n/1.5)^2$.

absence of FVa (second column in Table 1A) and in the absence of LUV (third and fourth columns in Table 1A). The K_m value is apparently above the testable concentration range for prothrombin in the absence of LUV. In fact, the rate constant decreases with increasing concentrations of FXa and substrate, possibly because of aggregation.

Initial rates, at <10% conversion, were measured at ~4−8 × 10^{-6} M (~4−8 K_m) in the presence of LUV and FXa/FVa = 1:4, and the slope of the lines, as in the example shown in Figure 2, gave the initial velocities. Table 1B shows k_{cat} values calculated from the average of three to four repeats of velocity measurements and the KSIE under a variety of conditions. The KSIEs on k_{cat} became increasingly inverse, 0.30 ± 0.05 and 0.19 ± 0.04 (first and second columns in Table 1A), as the prothrombin concentration was increased to 4.0 × 10^{-6} M (~4 K_m) and 6.8 × 10^{-6} M (~6.8 K_m), respectively. On the other hand, initial rate studies gave a KSIE of 1.56 ± 0.31, when the FXa/FVa ratio was 1:1 and approaching 2.0, but with poor precision, when the LUV concentration was raised to 2 × 10^{-3} M and the FXa/FVa ratio was 1:1 (not shown). In the absence of FVa (fourth column in Table 1A), the k_{cat} values drop precipitously and the KSIE is still inverse.

FXa-Catalyzed Hydrolysis of Chromogenic Substrates. KSIEs for the bovine FXa-catalyzed hydrolysis of S-2288 were measured for V_{max} and V_{max}/K_m to be 2.39 ± 0.53 and 1.76 ± 0.19, respectively, at a 1.9 × 10^{-9} M enzyme concentration, at the pH of the maximal rate, 8.40 and equivalent pL, 0.020 M Tris, 0.30 M NaCl, and 5×10^{-3} M $CaCl_2$. The Michaelis−Menten constants are close to the values provided by Diapharma Co. under nearly identical conditions. The proton inventory for V_{max} for the bovine FXa-catalyzed hydrolysis of S-2288 is shown in Figure 3.

Full-progress curves were obtained with S-2765 = 1.0 × 10^{-3} M (4 K_m) at 445 nm, and the integrated Michaelis−Menten equation (*38*) was fitted to the 1000 absorbance−time pairs for two runs to obtain the k_{cat} values used for the proton-inventory curve in Figure 4. Values for k_{cat}/K_m were obtained from these calculations with large errors but gave a similar proton inventory to the one obtained from pseudo-first-order rate studies, conducted at 405 nm and 2.0 × 10^{-5} M S-2765, shown in Figure 4.

Model Selection for the Evaluation of Proton-Inventory Data. As detailed previously (*30*, *31*), we developed a protocol based on the Gross−Butler equation (*18*, *19*, *25*, *41*, *42*) given below, which relates the dependence of a particular rate parameter to the atom fraction of deuterium, *n*, in the solvent mixtures

$$V_n = V_o \prod_i^{TS} (1 - n + n\phi_i^T) / \prod_j^{RS} (1 - n + n\phi_j^R) \quad (1)$$

where V_n and V_o are velocities (or rate constants) in a binary solvent and water, respectively, *n* is the atom fraction of deuterium, RS is the reactant state, ϕ^R is the RS fractionation factor, and ϕ^T is the TS fractionation factor. The TS product

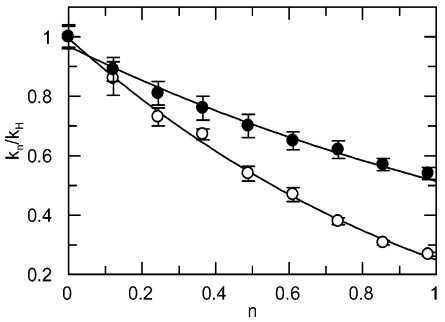

FIGURE 4: Ratios of rate constants measured in mixed isotopic water over the rate constants measured in water plotted against the atom fraction of deuterium, *n*, for the FXa-catalyzed hydrolysis of S-2765 at pH 8.40 and equivalent pL, 0.020 M Tris buffer, 0.30 M NaCl, 5×10^{-3} M $CaCl_2$, and 0.1% PEG-4000 at 25.0 ± 0.1 °C. (○) k_{cat} data, and the equation of the line is $k_n/k_H = 1.0(1 - n + n/1.75)^2 0.78^n$. (●) k_{cat}/K_m, and the equation of the line is $k_n/k_H = 1.0(1 - n + n/1.37)^2$.

is over TS fractionation factors, and the RS product is over RS fractionation factors. The fractionation factors can be perceived as inverse equilibrium isotope effects, K_D/K_H, for exchange between a bulk water site and a particular structural site of RS or TS. The most common simplifications of this equation involve the assumption of a unit fractionation factor of RS for catalytic residues with NH and OH functional groups and the assumption that one or two active-site units contribute in most hydrolytic enzymes. On the basis of our extensive experience with these systems, we fitted a variety of modifications of eq 1 to the data (see the Supporting Information) and accepted the model that gave the smallest reduced χ^2 value and TS fractionation factors that are most consistent with both the k_{cat}/K_m and k_{cat} proton inventories. We calculated a single exponential term for a generalized solvent rearrangement (regardless of its origin) (*19*, *29*), symbolized by ϕ_S^n, as best justified by past evidence (*31*, *43*).

DISCUSSION

There is an increasing appreciation of the critical role of the water structure in enzyme-catalyzed reactions (*44*, *45*). In light of this, KSIE and proton-inventory studies on the hydrolysis of natural substrates catalyzed by FXa seemed a worthwhile effort. Our study of the thrombin-catalyzed hydrolysis of two large natural protein substrates has shown a substantial role of solvent reorganization at the rate-limiting TS of these reactions (*30*). Because the catalytic activity of FXa is more medium-dependent than that of related enzymes studied to date, the activation of prothrombin is a unique target for studying the role of the water structure in catalysis. Prothrombin activation at the aqueous−lipid interface is pivotal in the regulation of blood coagulation. Once the components of the prothrombin complex are surface-bound, chemical transformations can occur at optimal speed. The process is associated with solvent restructuring, and thus, the physiological reaction catalyzed by FXa seems likely to show a strong contribution from solvent rearrangement. However, the challenge in kinetic measurements at the lipid−aqueous interface is not to be underestimated (*36*, *37*, *40*, *46*). To ensure consistency, buffered light and heavy water solutions of the reaction mixtures were made by dilution of common stock solutions in an identical manner. The extrusion of vesicles was performed with great care to achieve uniform size (*46*).

Human Factor Xa-Catalyzed Activation of Prothrombin. The critical physiological role of FXa is the activation of prothrombin to thrombin. A general reaction scheme (Scheme 1) has been suggested, which explains the observation of the occurrence of active meizothrombin in the presence of membranes and FVa (*7*, *36*, *37*).

At prothrombin concentrations well below K_m, the KSIEs are slightly inverse even in the absence of FVa and LUV. Wu et al. reported that the rate of the consecutive steps are comparable in the presence of FVa, $\sim 5 \times 10^{-5}$ M LUV, and prothrombin concentrations below K_m (*37*). However, the substrate dependence of the rate of FXa-catalyzed prothrombin activation varies at LUV concentrations of $2-5 \times 10^{-5}$ M. The Michaelis−Menten parameters for prothrombin activation depend upon the composition of the medium, which makes comparisons difficult. The K_m value was reported to be 200 times greater in the absence of FVa and LUV than in their presence (*37*). Our data displayed in Table 1A fully support these findings, as the second-order rate constants decline precipitously in the absence of FVa and LUV. Although the reaction path changes with the medium, on the basis of the KSIE values <1.0, the chemical steps are not rate determining when the enzyme is not saturated with substrate and/or does not operate at optimal activity. The intervention of meizothrombin can only be demonstrated at high prothrombin concentrations; otherwise, it is channeled to thrombin without release from the membrane−enzyme complex (*9*, *14*, *47*). The observed KSIEs in Table 1B reflect this observation in an interesting manner. KSIEs turn increasingly inverse, 0.30 ± 0.05 and 0.19 ± 0.04, indicating the predominance of a physical phenomenon as prothrombin concentrations increase. This is consistent with the proposal that meizothrombin accumulates with enhanced prothrombin concentrations, and the overall rate is limited by either binding or a conformational change to poise the Arg^{322}−Ile^{323} bond for cleavage. A conformational change was deemed necessary for the exposure and optimal projection of proteolytic sites in prothrombin (*16*, *47*). Amino acids near the carboxyl segment of FVa heavy chain and FXa exosites bind prothrombin to exert the necessary structural reassembly for catalysis (*10*, *12*). This transformation seems to be associated with an increase in the fractionation factors to 3.3−5.0, because of the reorganization of myriads of solvating water molecules. In contrast, the observation of a KSIE of 2.0 at 2×10^{-3} M LUV is consistent with a different rate-determining step, most likely, the formation of meizothrombin followed by rapid conversion to thrombin. Under less than optimal conditions, the chemical reactions leading to the formation of meizothrombin slow down.

Human Factor Xa-Catalyzed Hydrolysis of Tripeptide Anilides. Clearly, the contribution of TS proton bridges at the catalytic site of FXa cannot be assessed from studies of the FXa activation of prothrombin. Peptide-4-nitroanilide mimics of natural FXa substrates are ideal for this purpose. The chosen chromogenic tripeptides have the preferred Arg at the carboxyl side of the scissile bond, and each carries preferred P_2 and P_3 residues. The KSIEs and proton inventories for the FXa-catalyzed hydrolysis of these substrates bespeak of very different types of proton bridges, forming at the TS in the rate-determining step of peptide

Scheme 1: Thrombin Production from Human Prothrombin: The Balance of the Pathways on the Left and Right Is a Function of Conditions (*7*, *36*, *37*)

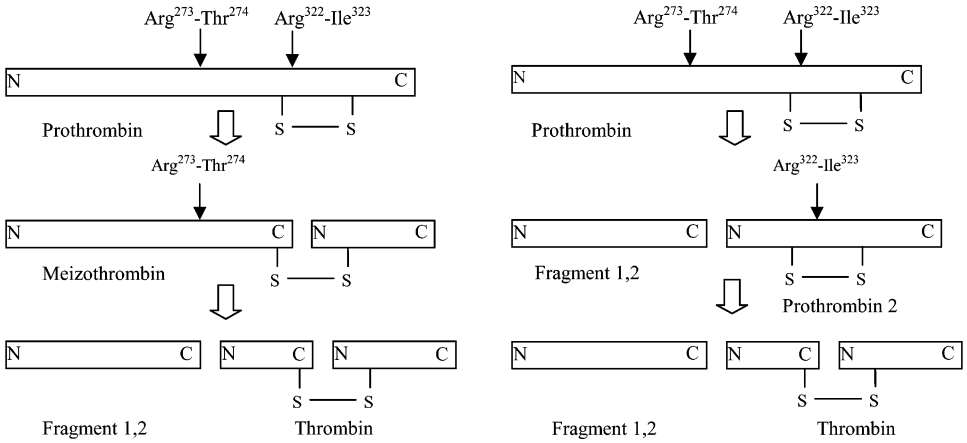

hydrolysis, than the proton bridge originating from solvent restructuring. Both S-2288 and S-2765 present concave proton inventories when they saturate the enzyme, indicative of multiproton participation at the TS: (1) For k_{cat} for S-2288, the fractionation factors obtained from the best statistical fit are (models and results of fits are provided in the Supporting Information) $\phi_1 = \phi_2 = 0.674 \pm 0.001$, indicating two equal proton bridges forming at the TS; KSIE = 1.48 each. (2) For k_{cat} for S-2765, a very good substrate of FXa, $\phi_1 = \phi_2 = 0.57 \pm 0.07$, indicating two equal proton bridges forming at the TS, and $\phi_S = 0.78 \pm 0.16$ for solvent restructuring. The curvature observable in Figure 4 arises from both, two proton bridges formed at the TS, each associated with a KSIE of 1.69 and a normal SIE originating from the reorganization of countless solvent molecules. Two proton bridges may also occur at the rate-determining TS for S-2765 below enzyme saturation with the substrate (k_{cat}/K_m), as measured with pseudo-first-order kinetics, but their strength cannot be established with certainty. Thus, unambiguous statistical distinction between the two-proton model with $\phi_1 = \phi_2 = 0.73 \pm 0.01$ and one with a strong contribution of solvent rearrangement, $\phi_S = 0.52 \pm 0.07$, while ϕ_1 or $\phi_1 = \phi_2 = 1.0 \pm 0.2$ is not possible in the latter case. Very good substrates of thrombin have also shown differences in fractionation factors depending upon enzyme saturation with the substrate. The TS fractionation factor is often at unity under k_{cat}/K_m conditions, which is consistent with a rate-determining physical step (binding or conformational change) associated with solvent reorganization rather than rate-determining chemical steps. In any case, the rate-determining step is likely to be different when FXa is not saturated with S-2765 from when it is, because the fractionation factors are quite different.

The assignment of the TS fractionation factors to the participation of proton bridges solely in the breakdown of the tetrahedral intermediate occurring in acylation or the formation of the tetrahedral intermediate in the hydrolysis of the acyl enzyme is uncertain. Their weighted average may be the most realistic account of the rate-determining TS: one or the other may dominate of course. The contribution of solvent rearrangement at the TS of the rate-determining step when FXa is saturated with S-2765 most likely indicates partial rate-determining leaving-group departure accompanied by solvent reorganization. This has also been seen with the thrombin-catalyzed hydrolysis of two highly specific substrate mimics (*31*).

The extent and nature of P and P′ sites in effectors of thrombin have a key role in mobilizing proton bridges at the rate-determining TS in acylation of the enzyme. Simple dipeptide amides invoke the participation of a single proton, while longer and more specific substrates recruit two or multiproton participation in the formation of proton bridges at the TS. This is in accordance with the efficiency of peptide bond cleavage indicated by the magnitude of k_{cat}/K_m (*17*, *23*). Schowen's hypothesis (*18*, *20*, *24*−*27*) that subsites on peptide substrates exert a compression to elicit contraction of the distance between proton donors and acceptors in acid−base catalytic pairs at the active site of enzymes is validated by the thrombin and FXa-catalyzed reactions and many previous protease-catalyzed reactions. H NMR signals of short strong hydrogen bonds (SSHBs) forming at the active site in serine hydrolases (*48*), including pancreatic proteases (*49*−*53*) and other enzymes, (*54*−*58*) when modified by mechanism-based inhibitors, have also been broadly studied and discussed. Proton transfer in these general-acid−base-catalyzed steps may be mediated by an SSHB at the TS (*21*). Our present results with FXa-catalyzed hydrolysis of tripeptide pNA complement and support these perceptions.

The chief conclusion of these KSIE and proton-inventory studies is that the rate-determining process in the FXa-catalyzed activation of prothrombin at the aqueous−lipid interface is dominated by physical events, most likely a conformational change accompanied by rearrangement of the water structure while poising the scissile bond for nucleophilic attack by Ser. In contrast, when the chemical steps are revealed, as in the FXa-catalyzed hydrolysis of highly effective tripeptide 4-nitroanilides, multiproton bridges are observed at the rate-determining TS: these are well-established properties of the active site of evolutionarily well-developed serine hydrolases.

SUPPORTING INFORMATION AVAILABLE

A total of 2 figures and 14 tables of kinetic rate constants and their ratios for KSIEs and proton inventories. This material is available free of charge via the Internet at http://pubs.acs.org.

REFERENCES

1. Furie, B., and Furie, B. C. (1988) The Molecular Basis of Blood Coagulation, *Cell 53*, 505−518.
2. Davie, E. W., Fujikawa, K., and Kisiel, W. (1991) The Coagulation Cascade: Initiation, Maintenance, and Regulation, *Biochemistry 29*, 10363−10370.
3. Mann, K. G., and Lorand, L. (1993) Introduction: Blood Coagulation, *Methods Enzymol. 222*, 1−10.
4. Patthy, L. (1993) Modular Design of Proteases of Coagulation, Fibrinolysis, and Complement Activation: Implications for Protein Engineering and Structure−Function Studies, *Methods Enzymol. 222*, 10−22.
5. Brandstetter, H., Kuhne, A., Bode, W., Huber, R., der Saal, W., Wirthensohn, K., and Engh, R. A. (1996) X-ray Structure of Active Site-Inhibited Clotting Factor Xa. Implications for Drug Design and Substrate Recognition, *J. Biol. Chem. 271*, 29988−29992.
6. Padmanabhan, K., Padmanabhan, K. P., Tulinsky, A., Park, C. H., Bode, W., Huber, R., Blankenship, D. T., Cardin, A. D., and Kisiel, W. (1993) Structure of Human des(1−45) Factor Xa at 2.2 Å Resolution, *J. Mol. Biol. 232*, 947−966.
7. Rosing, J., Tans, G., Govers-Riemslag, J. W., Zwaal, R. F., and Hemker, H. C. (1980) The Role of Phospholipids and Factor Va in the Prothrombinase Complex, *J. Biol. Chem. 255*, 274−283.
8. Husten, E. J., Esmon, C. T., and Johnson, A. E. (1987) The Active Site of Blood Coagulation Factor Xa. Its Distance from the Phospholipid Surface and Its Conformational Sensitivity to Components of the Prothrombinase Complex, *J. Biol. Chem. 262*, 12953−12961.
9. Carlisle, T. L., Bock, P. E., and Jackson, C. M. (1990) Kinetic Intermediates in Prothrombin Activation. Bovine Prethrombin 1 Conversion to Thrombin by Factor X, *J. Biol. Chem. 265*, 22044−22055.
10. Nesheim, M. E., Foster, W. B., Hewick, R., and Mann, K. G. (1984) Characterization of Factor V Activation Intermediates, *J. Biol. Chem. 259*, 3187−3196.
11. Bukys, M. A., Blum, M. A., Kim, P. Y., Brufatto, N., Nesheim, M. E., and Kalafatis, M. (2005) Incorporation of Factor Va into Prothrombinase Is Required for Coordinated Cleavage of Prothrombin by Factor Xa, *J. Biol. Chem. 29*, 27393−27401.
12. Beck, D. O., Bukys, M. A., Singh, L. S., Szabo, K. A., and Kalafatis, M. (2004) The Contribution of Amino Acid Region Asp695−Tyr698 of Factor V to Procofactor Activation and Factor Va Function, *J. Biol. Chem. 279*, 3084−3095.
13. Rezaie, A. R., and Esmon, C. T. (1995) Contribution of Residue 192 in Factor Xa to Enzyme Specificity and Function, *J. Biol. Chem. 270*, 16176−16181.
14. Boskovic, D. S., Bajzar, L. S., and Nesheim, M. E. (2001) Channeling During Prothrombin Activation, *J. Biol. Chem. 276*, 28686−28693.
15. Kalafatis, M., Beck, D. O., and Mann, K. G. (2003) Structural Requirements for Expression of Factor Va Activity, *J. Biol. Chem. 278*, 33550−33561.
16. Vijayalakshmi, J., Padmanabhan, K. P., Mann, K. G., and Tulinsky, A. (1994) The Isomorphous Structures of Prethrombin2, Hirugen-, and PPACK-Thrombin: Changes Accompanying Activation and Exosite Binding to Thrombin, *Protein Sci. 3*, 2254−2271.
17. Hedstrom, L. (2002) Serine Protease Mechanism and Specificity, *Chem. Rev. 102*, 4501−4524.
18. Alvarez, F. J., and Schowen, R. L. (1987) Mechanistic Deductions from Solvent Isotope Effects. In *Isotopes in Organic Chemistry* (Buncel E., and Lee, C. C., Eds.) Elsevier, Amsterdam, The Netherlands.
19. Kresge, A. J., More, O., and Powell, M. F. (1987) Solvent Isotopes Effects, Fractionation Factors and Mechanisms of Proton Transfer Reactions. In *Isotopes in Organic Chemistry* (Buncel E., and Lee, C. C., Eds.) Elsevier, Amsterdam, The Netherlands.
20. Schowen, R. L. (1988) Structural and Energetic Aspects of Protolytic Catalysis by Enzymes: Charge-Relay Catalysis in the Function of Serine Proteases. In *Mechanistic Principles of Enzyme Activity* (Liebman J. F., and Greenberg, A., Eds.) VCH Publishers, New York.
21. Schowen, K. B., Limbach, H. H., Denisov, G. S., and Schowen, R. L. (2000) Hydrogen Bonds and Proton Transfer in General-Catalytic Transition State Stabilization in Enzyme Catalysis, *Biochem. Biophys. Acta. 1458*, 43−62.
22. Quinn, D. M., and Sutton, L. D. (1991) Theoretical Basis and Mechanistic Utility of Solvent Isotope Effects, In *Enzyme Mechanism from Isotope Effects* (Cook, P. F., Ed.) CRC Press, Boston, MA.
23. Fersht, A. (1999) *Structure and Mechanism in Protein Science*, W. H. Freeman and Co., New York.
24. Elrod, J. P., Hogg, J. L., Quinn, D. M., and Schowen, R. L. (1980) Protonic Reorganization and Substrate Structure in Catalysis by Serine Proteases, *J. Am. Chem. Soc. 102*, 5365−5376.
25. Venkatasubban, K. S., and Schowen, R. L. (1985) The Proton Inventory Technique, *CRC Crit. Rev. Biochem. 17*, 1−44.
26. Stein, R. L., Elrod, J. P., and Schowen, R. L. (1983) Correlate Variations in Enzyme-Derived and Substrate-Derived Structures of Catalytic Transition States. Implications for the Catalytic Strategy of Acyl-Transfer Enzymes, *J. Am. Chem. Soc. 105*, 2446−2452.
27. Stein, R. L., Strimpler, A. M., Hori, H., and Powers, J. C. (1987) Catalysis by Human Leukocyte Elastase: Proton Inventory as a Mechanistic Probe, *Biochemistry 26*, 1305−1314.
28. Scholten, J. D., Hogg, J. L., and Raushel, F. M. (1988) Methyl Chymotrypsin Catalyzed Hydrolysis of Specific Substrate Esters Indicate Multiple Proton Catalysis Is Possible with a Modified Charge Relay Triad, *J. Am. Chem. Soc. 110*, 8246−8247.
29. Chiang, Y., Kresge, A. J., Chang, T. K., Powell, M. F., and Wells, J. A. (1995) Solvent Isotope Effects on a Hydrolysis Reaction Catalyzed by Subtilisin and Its N155G Mutant−Failure of the Proton Inventory Method To Report Hydrogen-Bonding Interactions in the Oxyanion Hole, *J. Chem. Soc., Chem. Commun.* 1587−1588.
30. Zhang, D., and Kovach, I. M. (2005) Full and Partial Deuterium Solvent Isotope Effect Studies of α-Thrombin-Catalyzed Reactions of Natural Substrates, *J. Am. Chem. Soc. 127*, 3760−3766.
31. Enyedy, E. J., and Kovach, I. M. (2004) Proton Inventory Studies of Thrombin-Catalyzed Reactions of Substrates with Selected P and P′ Sites, *J. Am. Chem. Soc. 126*, 6017−6024.
32. Schellenberger, V., Turck, C. W., and Rutter, W. J. (1994) Role of the S′ Subsites in Serine Protease Catalysis. Active-Site Mapping of Rat Chymotrypsin, Rat Trypsin, α-Lytic Protease, and Cercarial Protease from *Schistosoma mansoni*, *Biochemistry 33*, 4251−4257.
33. Schellenberger, V., Turck, C. W., Hedstrom, L., and Rutter, W. J. (1993) Mapping the S′ Subsites of Serine Proteases Using Acyl Transfer to Mixtures of Peptide Nucleophiles, *Biochemistry 32*, 4349−4353.
34. Le Bonniec, B. F., Myles, T., Johnson, T., Knight, C. G., Tapparelli, C., and Stone, S. R. (1996) Characterization of the P_2' and P_3' Specificities of Thrombin Using Fluorescence-Quenched Substrates and Mapping of the Subsites by Mutagenesis, *Biochemistry 35*, 7114−7122.
35. Dai, Y., Hedstrom, L., and Abeles, R. H. (2000) Inactivation of Cystein Proteases by (Acyloxy) Methyl Ketones Using S′−P′ Interactions, *Biochemistry 39*, 6498−6502.
36. Banerjee, M., Majumder, R., Weinreb, G., Wang, J., and Lentz, B. R. (2002) Role of Procoagulant Lipids in Human Prothrombin Activation. 2. Soluble Phosphatidylserine Upregulates and Directs Factor X(a) to Appropriate Peptide Bonds in Prothrombin, *Biochemistry 41*, 950−957.
37. Wu, J. R., Zhou, C., Majumder, R., Powers, D. D., Weinreb, G., and Lentz, B. R. (2002) Role of Procoagulant Lipids in Human Prothrombin Activation. 1. Prothrombin Activation by Factor X(a) in the Absence of Factor V(a) and in the Absence and Presence of Membranes, *Biochemistry 41*, 935−949.
38. Goudar, C. T., Sonnad, J. R., and Duggleby, R. G. (1999) Parameter Estimation Using a Direct Solution of the Integrated Michaelis−Menten Equation, *Biochim. Biophys. Acta 1429*, 377−383, and references therein.
39. Leatherbarrow, R. J. (1992) *GraFit User's Guide*, Ertihacus Sofware Ltd., Staines, U.K.
40. Chen, L., Yang, L., and Rezaie, A. R. (2003) Proexosite-1 on Prothrombin Is a Factor Va-Dependent Recognition Site for the Prothrombinase Complex, *J. Biol. Chem. 278*, 27564−27569.
41. Gold, V. (1969) Protolytic Processes in H_2O-D_2O Mixtures, *Adv. Phys. Org. Chem. 7*, 259−331.
42. Kresge, A. J. (1964) Solvent isotope effects in H_2O-D_2O Mixtures, *Pure Appl. Chem. 8*, 243−258.
43. Stein, R. L. (1985) Transition-State Properties for the Association of α-1-Protease Inhibitor with Porcine Pancreatic Elastase, *J. Am. Chem. Soc. 107*, 6039−6042.

44. Park, C., and Raines, R. T. (2001) Quantitative Aanalysis of the Effect of Salt Concentration on Enzyme Catalysis, *J. Am. Chem. Soc. 123*, 11472−11479.
45. Ru, M. T., Hirokane, S. Y., Lo, A. S., Dordick, J. S., Reimer, J. A., and Clark, D. S. (2000) On the Salt-Induced Activation of Lyophilized Enzymes in Organic Solvents: Effect of Salt Kosmotropicity on Enzyme Activity, *J. Am. Chem. Soc. 122*, 1565−1571.
46. Mayer, L. D., Hope, M. J., and Cullis, P. R. (1986) Vesicles of Variable Sizes Produced by a Rapid Extruison Procedure, *Biochem. Biophys. Acta 858*, 161−168.
47. Chattopadhyay, A., James, H. L., and Fair, D. S. (1992) Molecular Recognition Sites on Factor Xa which Participate in the Prothrombinase Complex, *J. Biol. Chem. 267*, 12323−12329.
48. Mildvan, A. S., Massiah, M. A., Harris, T. K., Marks, G. T., Harrison, D. H. T., Viragh, C., Reddy, P. M., and Kovach, I. M. (2002) Short Strong Hydrogen Bonds on Enzymes: NMR and Mechanistic Studies, *J. Mol. Stucture. 215*, 163−175.
49. Frey, P. A., Whitt, S. A., and Tobin, J. B. (1994) A Low-Barrier Hydrogen Bond in the Catalytic Triad of Serine Proteases, *Science 264*, 1927−1930.
50. Tobin, J. B., Whitt, S. A., Cassidy, C. S., and Frey, P. A. (1995) Low-Barrier Hydrogen Bonding in Molecular Complexes Analogous to Histidine and Aspartate in the Catalytic Triad of Serine Proteases, *Biochemistry 34*, 6919−6924.
51. Cassidy, C. S., Lin, J., and Frey, P. A. (1997) A New Concept for the Mechanism of Action of Chymotrypsin: The Role of the Low-Barrier Hydrogen Bond, *Biochemistry 36*, 4576−4584.
52. Lin, J., Westler, W. M., Cleland, W. W., Markley, J. L., and Frey, P. A. (1998) Fractionation Factors and Activation Energies for Exchange of the Low Barrier Hydrogen Bonding Proton in Peptidyl Trifluoromethyl Ketone Complexes of Chymotrypsin, *Proc. Natl. Acad. Sci. U.S.A. 95*, 14664−14668.
53. Lin, J., Cassidy, C. S., and Frey, P. A. (1998) Correlations of the Basicity of His 57 with Transition State Analogue Binding, Substrate Reactivity, and the Strength of the Low-Barrier Hydrogen Bond in Chymotrypsin, *Biochemistry 37*, 11940−11948.
54. Halkides, C. J., Wu, Y. Q., and Murray, C. J. (1996) A Low-Barrier Hydrogen Bond in Subtilisin: ^{1}H and ^{15}N NMR Studies with Peptidyl Trifluoromethyl Ketones, *Biochemistry 35*, 15941−15948.
55. Ash, E. L., Sudmeier, J. L., De Fabo, E. C., and Bachovchin, W. W. (1997) A Low-Barrier Hydrogen Bond in the Catalytic Triad for Serine Proteases? Theory Versus Experiment, *Science 278*, 1128−1132.
56. Kahayaoglu, A., Haghjoo, K., Guo, F., Jordan, F., Kettner, C., Felfoldi, F., and Polgar, L. (1997) Low Barrier Hydrogen Bond Is Absent in the Catalytic Triads in the Ground State but Is Present in a Transition-State Complex in the Prolyl Oligopeptidase Family of Serine Proteases, *J. Biol. Chem. 272*, 25547−25554.
57. Bao, D., Huskey, P. W., Kettner, C. A., and Joradn, F. (1999) Hydrogen Bonding to Active-Site Histidine in Peptidyl Botonic Acid Inhibitor Complexes of Chymotrypsin and Subtilisin: Proton Magnetic Resonance Assignments and H/D Fractionation, *J. Am. Chem. Soc. 121*, 4684−4689.
58. Massiah, M. A., Viragh, C., Reddy, P. M., Kovach, I. M., Johnson, J., Rosenberry, T. L., and Mildvan, A. S. (2001) Short, Strong Hydrogen Bonds at the Active Site of Human Acetylcholinesterase: Proton NMR Studies, *Biochemistry 40*, 5682−5690.

BI061218M